A New Cone Beam X-Ray Microtomography Facility for 3D Analysis of Multiphase Materials

C. L. Lin and J. D. Miller

Department of Metallurgical Engineering, University of Utah,
135 South 1460 East, Room 412, Salt Lake City, Utah 84112, E-mail: {cllin, jdmiller}@mines.utah.edu

ABSTRACT

Three-dimensional x-ray microtomography offers a unique imaging capability. Spatial resolution on the order of ten microns can be achieved with the use of microfocus x-ray generators. Recently, a state-of-the-art, flexible cone beam x-ray microtomography system has been installed at the University of Utah for the quantitative analysis of multiphase materials in three dimensions. With the use of 2D cone beam projections rather than 1D slice projections the amount of wasted radiation is reduced. The custom designed facility has the capacity to obtain 2048 x 2048 pixel reconstruction over a 10-mm diameter, while also allowing for the imaging of somewhat larger (40-mm) objects. The system is capable of handling high-density materials, even materials having a density as high as 8.0 g/cm^3. This unique, one-of-a-kind, instrument will be used to obtain three-dimensional spatial reconstruction for such applications as 3D-liberation analysis, structural examination of particle beds/porous structures, and the examination of air-void systems in concrete structures. The utilization of x-ray microtomography not only will allow for quantitative analysis of multiphase systems but also will allow for textural characterization and the determination of phase continuity. In this paper, we present information regarding the current use of this new facility and review potential applications for this advanced analytical system.

Keywords Cone Beam, X-ray Microtomography, 3D Analysis

1 INTRODUCTION

Medical and industrial applications of computed tomography systems have been proven over the last several years. The ability to map multiphase systems in three dimensions has revolutionized diagnostic analysis in many areas of technology. However, CT systems have not yet been widely applied to the analysis of microsystems because of resolution limitations. There is considerable interest in applying three-dimensional tomographic imaging to study the microstructure of various materials including metal, rock, mineral, ceramics, composites, microelectromechanical system (MEMS), chips, and bone architecture. Specifically, structural and textural features of irregular geometry cannot be characterized/determined from conventional two-dimensional microscopy of polished sections. This includes determination of compositional distribution for irregularly shaped composite particles, cracking and delamination of critical interfaces, and the interconnected network of porous microstructures.

New techniques for improving productivity and efficiency are the key to success in today's highly competitive market place. For continued technological progress in the fields of mineral processing and materials research, the need for non-destructive quantitative spatial analysis of material/devices in three-dimensions has increased significantly. Such quantitative information must be accurate enough so that the measured values can be used as parameters for simulation models, process design procedures, and control strategies. In this regard, x-ray microtomography offers a unique capability to image multiphase systems in three dimensions. Spatial resolution on the order of ten microns can be achieved with the use of microfocus x-ray generators. For example, high-resolution x-ray microtomography can be used for the direct determination of the three-dimensional liberation spectrum of multiphase particles several 100 microns in size from mineral processing streams.

1.1 X-ray Tomography Background

The first discovery of x-rays by Roentgen in 1895 provided a new imaging technique. The primary advantage of x-ray radiography is the capability to penetrate thick, intact, and wet samples with natural contrast. At present, radiography is used for inspection of materials in many applications. It is noted

that overlaying structures are ambiguous in their physical location using conventional radiography. This problem can be solved by the use of tomographic techniques.

Image reconstruction from projections using computed tomography (CT) produces a noninvasive measure of structure from external measurements. In x-ray CT, radiation is passed along straight lines through the object to a detector. The specimen is located between the source and detector. The source and detector are stationary as the specimen is rotated. Then is stopped at predetermined locations to acquire projections through the specimen. The projected signal are proportional to the amount of radiation reaching the detector. The logarithm of these measurements can be considered line integrals of the x-ray attenuation coefficients of the specimen. Knowledge of all line integrals allows the reconstruction of the interior structure (Kak and Slaney, 1987). X-ray tomographic reconstruction produces a two-dimensional map of x-ray attenuation coefficients of the irradiated cross section of the specimen. Differentiation of features within the sample is possible because the linear attenuation coefficient (μ) at each point depends directly on the electron density, the effective atomic number (Z) of the material comprising the sample, and the energy of the x-ray beam (E). A simplified equation that illustrates the approximate relationship among these quantities is

$$\mu = \rho\left(a + \frac{bZ^{3.8}}{E^{3.2}}\right) \tag{1}$$

where ρ is the density of the phase, a is a quantity with a relatively small energy dependence and b is a constant (McCullough, 1975; Wellington and Vinegar, 1987). When a mixture of atomic species is present, Z (the effective atomic number) is defined by

$$Z^{3.8} = \sum_i \left(f_i [Z_i]^{3.8}\right) \tag{2}$$

where f_i is the fraction of the total number of electrons contributed by element i with atomic number Z_i. For the case of transmission tomography such as x-ray CT, the modern CT scanners are capable of discriminating between values of μ that differ by as little as 0.1%. Different mineral phases which may be contained inside a host ore body can be discriminated easily using the x-ray CT technique. In practice, density measurement from x-ray tomographic data can be done either by calibrating the CT machines with objects of known density and obtaining a correlation equation that relates density with attenuation coefficients or using dual energy scanning to determine directly the density of the material. In such a fashion, then, a two-dimensional density map of the object under investigation can be established.

Typically volumetric imaging of the sample is obtained by stacking a series of two-dimensional slices of CT image data. It should be noted that the quality and utility of the CT data ultimately depends on the resolution of the machine employed. Medical x-ray CT systems have a beam width of a few millimeters and an energy source of about 130 keV x-rays. Generally, such a system would not be adequate for many applications such as liberation analysis of mineral particles several hundred microns in size as are of interest in mineral processing operations.

1.2 High-Resolution Three-Dimensional X-ray Microtomography

The application of the principles of CT at the microscale level, or microtomography, allows quantitative investigation of objects in three dimensions. Only recently, practical microtomography systems have been developed. Early microtomography systems produced 2D images. Some current systems, including the one described here, produces true 3D image data. In addition to electron impact x-ray sources, x-rays from synchrotrons have also been used in microtomography. Spatial resolution of the order of 1 μm and 15 μm can be achieved with the use of synchrotron radiation (Grodzins, 1983; Flannery et al., 1987; Kinney et al., 1988) and conventional microfocus x-ray generators (Feldkamp and Jesion, 1986; Kinney et al., 1991; Dunsmuir et al., 1991).

As the resolution and the techniques for 3-D geometric analysis have advanced in the last decade, it is now possible to map in detail the mineralogical texture of ore particles in three-dimensional digital space. It is expected that the mineral phases inside particles should be described in three dimensions with micrometer resolution. In this regard, three-dimensional x-ray microtomography offers a unique

imaging capability. Spatial resolution on the order of 10 microns can be achieved with the use of microfocus x-ray generators.

For many years, the standard method of acquiring a volumetric CT scan has been by scanning a sample one slice at a time. In this method, a linear detector array and an x-ray point source are mounted opposite each other. A fan-shaped x-ray beam traverses the sample and the attenuated fan is stored as a 1-D linear image. By rotating the source/detector pair around the sample, a series of linear images are obtained which are subsequently used for the 2-D slice reconstruction. A volumetric representation is obtained by advancing the table on which the sample rests after each rotation in order to acquire a stack of such slices. Figure 1 shows the approach of traditional "slice by slice" tomography.

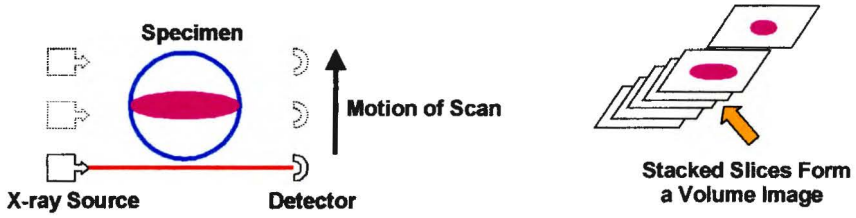

Figure 1: Volume Reconstruction from traditional "slice by slice" tomography

The problem with this approach is three-fold:

- Projection data covering sample regions between the thin slice sections is not available, which may account for missing small object information if the small object is located between two slices. As a consequence, the related spacing factor can not be accurately determined.
- The stop-and-go table movement may cause sample displacement between sequential scans, leading to slice misalignment in the volume reconstruction.
- Better lateral resolution is achieved when compared to axial resolution. The problem in image reconstruction is that the volume elements have different lateral and axial extents. This makes the reconstruction complicated and significantly inaccurate if the 3D reconstruction is to be used for quantitative purposes.

On the other hand, for cone-beam CT, a whole 3-D data set is acquired with only one rotation of the sample. This provides for fast data acquisition and better x-ray utilization. In a cone-beam design, each projection of the object is, in essence, a radiograph. Attenuation measurements are simultaneously made for the entire object rather than for a single slice. The reconstruction algorithm is a generalization in three dimensions of the widely used convolution-back projection method. Figure 2 shows a schematic diagram for the cone-beam geometry microtomography.

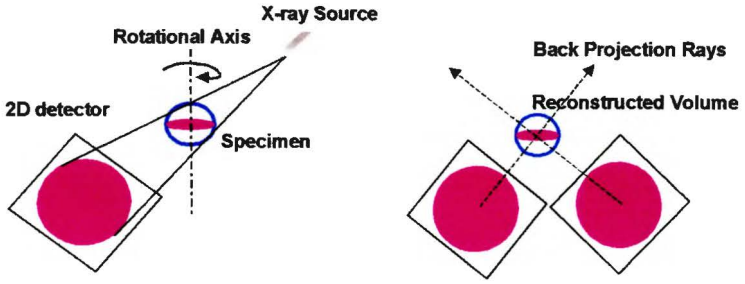

Figure 2: Volume reconstruction from cone-beam tomography

Clearly, cone-bean CT has the best prospects for true 3D liberation analysis and should be able to provide the necessary accuracy to quantitatively describe these micron-sized multiphase systems such as the 3D distribution of mineral phases in multiphase particles. One of only a few cone beam x-ray microtomography systems in the U.S. have now been installed in a dedicated laboratory at the

University of Utah. In this paper, we present information regarding the use of this new facility and review potential applications for advanced micro analysis of multiphase systems.

2 METHOD

2.1 X-ray Microtomography System Hardware

The state-of-the-art x-ray micro-CT machine, Konoscope 40-130 (cone beam geometry from ARACOR, Sunnyvale, CA), has been custom-designed, was installed (September 2000) and is now operating in a dedicated laboratory at the University of Utah. The Konoscope system has been designed based on the following considerations:

- a system geometry optimized to obtain high resolution 2D and 3D CT images of small samples but with the flexibility to examine larger objects as required,
- a detector with the resolution, efficiency and dynamic range required to obtain high quality data from a broad spectrum of samples,
- a reliable x-ray source which will allow us to focus on research rather than maintenance, and
- a high accuracy positioning system required to maintain the spatial resolution provided by the x-ray imaging component.

In this regard, the Konoscope system was designed and assembled to obtain 2048 x 2048 pixel reconstruction over a 10 mm diameter, while allowing for the imaging of somewhat larger (40 mm) objects. Specifically, the specimen positioning stage system can be manually mounted at one of three different locations, providing system magnifications of 5, 2 or 1.25 and spheres of reconstruction with respective diameters of 10 , 25 or 40 mm. Also, the system has been designed to be capable of handling high-density materials, even materials having a density as high as 8.0 g/cm^3.

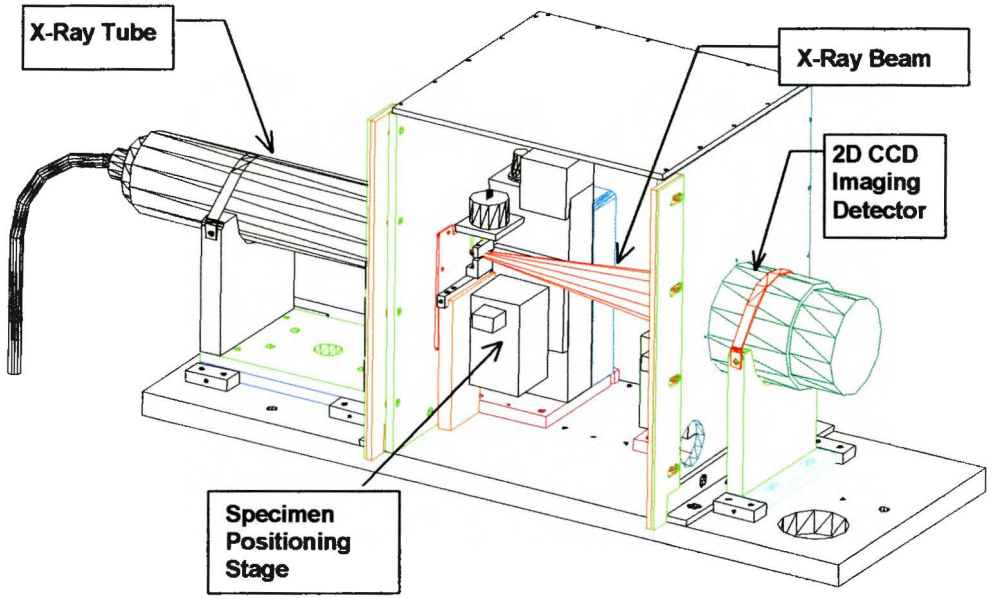

Figure 3: Schematic diagram of x-ray microtomography system (Konoscope 40-130)

The Konoscope system consists of a microfocus x-ray source, a specimen positioning stage, and a digital x-ray detection camera. These hardware components are integrated inside an interlocked radiation-safety enclosure. This container is mounted on a vibration-isolated stand which also supports the power-supplies, drivers and controllers for the x-ray source, CCD camera and positioning system. Figure 3 provides a perspective view of the system. A photograph of the cone beam x-ray microtomography system is shown in Figure 4. A Macintosh Power PC scan-control computer (with LabView/LVCam software) is used for control of image acquisition and specimen movement. At present, three image acquisition modes (radiograph, fan-beam and cone-beam geometry) can be

performed depending on the application. In the future, the system can be easily adapted with suitable scan-control and reconstruction software to perform the spiral or helical scan-geometry tomography. 3D tomographic images are reconstructed using an SGI Octane workstation (2 MIPS R12000 processors, 2Gigabyte of RAM).

Figure 4: The cone-beam x-ray microtomography system

2.1.1 X-ray source

The microfocus x-ray tube is a Kevex Model No. KM13006. The focal spot on the x-ray tube is 8 μm at 8 Watts and 20 μm at 16 Watts. In addition, a source filter is used to harden the spectrum which reduces beam-hardening artifacts and reduces the requisite dynamic range.

2.1.2 Specimen positioning stage

It is extremely important that the resolution of the system not be compromised by imprecise motion of the sample and variations in the location of the rotary and optical axes of the system. The combination of the rotary and translation motions must not move any point in the imaging volume out of place by more than a small fraction of the voxel size, i.e. a few microns. This requirement is particularly difficult for the vertical translation stage, both, because precise vertical translation is more difficult than precise rotary motion, and because the vertical translation axis must be exactly parallel to the rotary axis. A computer control vertical/rotary positioning system provides movement of the specimen in the x-ray beam. Sample mounting is accomplished via mounting holes to the rotary table top. As mentioned previously, the positioning system can be manually mounted at one of three different locations for different magnifications. Each time the system magnification is changed, a calibration routine needs to be used to locate the central axes of the system.

2.1.3 X-ray image detector

The x-ray image detection system consists of a fiberoptic taper, scintillator/fiberoptic faceplate, and Photometrics XR300 camera system with Thompson 2048x2048, Grade 1 CCD. Use of the scintillator with fiberoptic taper provides a estimated quantum efficiency of 66% at 80 keV according to the manufacturers. In addition, the detection system provides a 16-bit digitization at 200,000 pixels per second.

2.2 Procedure to Establish Scan Parameters

The following parameters must be established in order to start a scan: field-of-view (FOV), matrix size, number of views, size of the x-ray focal spot, source filter, operating voltage, integration time, stage position, and pixel parameters. The location of the positioning system is determined by the field-of-view and the required spatial resolution. The positioning system can be placed at three different positions (left, middle, right) depending on the desired field-of-view. Within each field-of-view, the spatial resolution can be set by the way that the CCD pixels are binned. Serial and parallel binning combine charges from adjacent pixels during readout. Binning is used to improve signal-to-noise ratio or to work at faster frame rates, but it decreases the lateral resolution of the image. Choosing a binning factor of 1 in both directions causes the CCD to read out the value in each pixel to assemble a 2048 x 2048 image. Choosing 2 in both directions causes the CCD to read the combined values of four pixels at a time to assemble a 1024 x 1024 image. Table 1 shows how the size of a pixel at the object position varies as a function of the binning factor and sample location. Table 2 shows how the estimated spatial resolution varies with sample location. In general, the number of detectors will equal the horizontal matrix size and the number of views should be about 70% to 100% of that number (otherwise if there are sharp features, streak artifacts will occur). The number of detectors is determined by how the CCD is binned (as shown in Table 1) and by the cropping of the detector field-of-view. The width of the detector field-of-view should be just large enough so that the image of the object is not clipped at any angular position during the scan.

Location	Magnification	Maximum Field-of-View (mm)	Pixel Size at Object (μm)		
			Bin = 4 (512^3)	Bin = 2 (1024^3)	Bin = 1 (2048^2)
Left	5	10	20	10	5
Middle	2	25	50	25	12.5
Right	1.25	40	80	40	20

Table 1: System parameters for full FOV reconstruction.

Location	Magnification	Spatial Resolution (μm)		
		Bin = 4 (512^3)	Bin = 2 (1024^3)	Bin = 1 (2048^2)
Left	5	40	22	18
Middle	2	100	55	45
Right	1.25	160	90	75

Table 2: Estimated spatial resolution.

2.3 Geometry Calibration of the System

The geometry of the system must be known for proper reconstruction. The geometry calibration is used to determine the magnification and distortion within the image that is done when the stage is moved or when the voltage on the x-ray tube is changed. These geometry calibration data are obtained by precisely moving a small ball over the field of view, while recording the location in the image. Three kinds of calibration sets are acquired for tomographic reconstruction. These data sets are for distortion, horizontal and vertical axes calibrations.

2.4 Scan Control Computer

The scan control computer (SCC) is an Apple Power Mac G3 equipped with Mac OS 8.6. The scan control program is a LabView application. Additional software has been provided for networking the SCC with the reconstruction workstation (SGI Octane).

2.5 Scan Procedures

Once the system is geometrically calibrated, the sample can be mounted on the rotary top stage and scans can be acquired. Scan procedures begin with the selection and entering of the scan parameters into the SCC. The first data sets that will be acquired are the air and offset scans. The offset scan quantifies the signal measured in the absence of x-rays and includes the dark current, which is proportional to the integration time, and the digitization offset, which is independent of the integration time. The air scan is the image obtained with the x-rays on, but without a sample in the field of view.

The non-uniformity in the air scan image includes effects of non-uniformities in the x-ray beam, non-uniform response of the scintillator, the structure of the fiber optic taper, and the non-uniform response of the CCD.

2.6 Reconstruction

Once the scans are completed, acquired scan data are transferred from the scan control computer (Mac) to the reconstruction workstation (SGI). There are two programs, system calibration and tomographic reconstruction, to perform calibration and reconstruction processes respectively.

3 High Resolution X-ray Microtomographic Applications

The essential feature of x-ray tomographic imaging is the determination of material density (more accurately attenuation coefficient) of a small region of three dimensional space called a voxel. Tomography can determine the density of all voxels in the three-dimensional region of the scan. Of course, the position of each voxel is known precisely. It is desired to determine the geometric characteristics of any region of space that is subject to variations in density. In particular it is possible to determine precisely the shape, and therefore volume, as well as the mass of each individual phase within the target volume. Examples of three applications are reviewed below.

3.1 Particle Composition Distribution (3D Liberation Analysis)

As mentioned previously, polished section techniques for the examination of the internal structures of particles are destructive and require lengthy experimental procedures. Recently the application of x-ray CT in mineral processing technology was reviewed (Miller et al., 1990; Lin et al., 1992). For quantitative analysis of particulate systems such as coal washability analysis, a recent study (Lin et al. 2000) indicated that a conventional medical x-ray CT scanner can provide sufficient information to construct the washability curve within minutes of sample collection. In fact, it now seems possible to design an on-line washability system for the control of coarse coal cleaning circuits.

For detailed liberation analysis, the volumetric grade distribution of multiphase mineral particles can be measured directly by cone-beam x-ray microtomography as described in previous study (Lin and Miller, 1996). High spatial resolution and the direct processing of raw volumetric data are the two important benefits offered by this new method. Figure 5 illustrates the ability of the high resolution x-ray microtomography (Konoscope) system for quantitative analysis to determine the 3D spatial distribution of mineral phases in multiphase particles. Four consecutive cross sections (from a total of 500 sections) along the Z-direction are shown as established from the three dimensional reconstruction of a phosphate rock sample. It should be noted that these sections are taken from the three dimensional image and not from a "slice by slice" approach mentioned early. The image elements in the reconstruction are cubic, so the spacing between planes equals the resolution which in the Z-direction corresponds to 20 μm. Here the gray scale levels of the images indicate the relative attenuation coefficient present in the bulk of the sample. Based on x-ray attenuation coefficient, differentiation of mineral phases within the sample is possible. For example, the x-ray attenuation coefficient histogram of the left-hand side image in Figure 6 is shown in the upper right-hand side. Several mineral phases are clearly identified from the peaks of the histogram. Furthermore, x-ray attenuation coefficients of individual voxels along the line are shown in the lower right-hand side of Figure 6.

Three dimensional liberation analysis by microtomography provides an excellent opportunity to overcome many of the limitations of currently used polished section techniques. With the x-ray microtomography system, complete accounting of the 3D spatial distribution of mineral phases in each particle is possible, including grain size distribution, interfacial area, shape features and textural information.

3.2 Pore Structure Analysis of Particle Beds During Filtration

Continuous filtration of fine particles involves filter cake formation and removal of surface moisture by drawing air through the porous structure. Accurate assessment of the transport properties of porous media (in our case filter cake) is of major importance in the development of improved filtration processes. Implications from these studies are important in the design and operation of filtration

equipment in order to enhance the efficiency of this important solid-liquid separation process. The microstructure and the connectivity of the pore space are important to describe fluid flow in filter cake during fine particle filtration. In this regard, characterization of pore structure based on parameters permitting inferences on the fluid balance is of particular interest. The pore structure has to be described by parameters which are of special relevance for the interpretation of fluid transport phenomena. These parameters should be based on directly measured variables of the pore system and not indirect variables (such as those determined empirically from transport processes) valid only for a particular pore structure. In this way fundamental relationships between pore structure and fluid transport at the microstructure level can be described. Thus, it is desired to be able to directly measure the three-dimensional interconnected pore structure of filter cake.

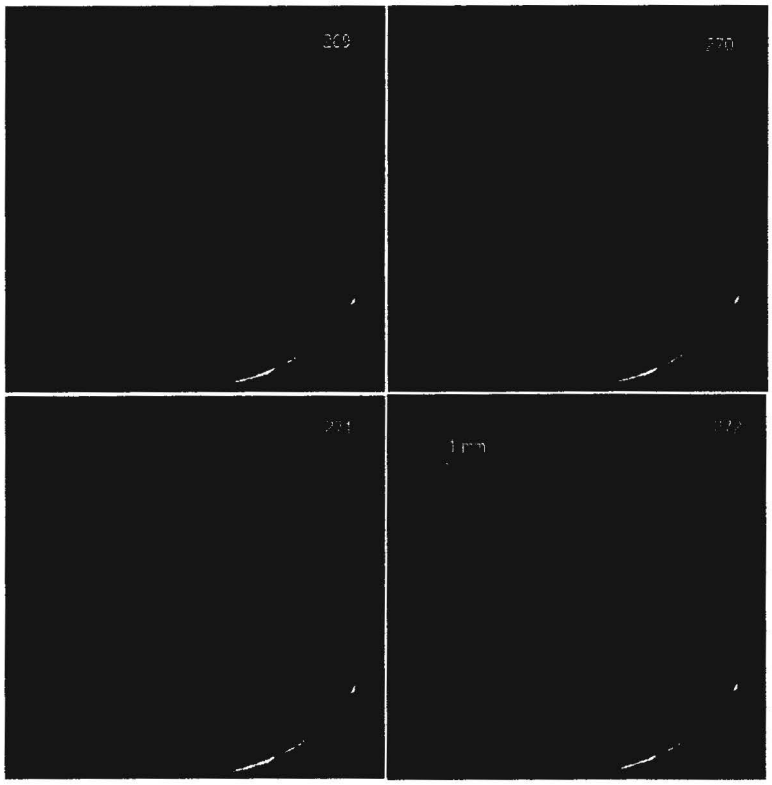

Figure 5: Cross sectional images from the three dimensional x-ray microtomography reconstruction of multiphase phosphate rock particles. The dark colored grains distinguish the phosphate mineral phase in a dolomite matrix

Most present methods to characterize the pore microstructure and its completed interconnected network rely on the microscopic observation of a series of thin or polished sections of the porous media. These data sets are then used to reconstruct and to display the three-dimensional image of the porous system with the help of advanced computer graphic techniques. Complete analysis of the 3-D porous system from serial sections is a tedious and time-consuming process. In addition, for a completely interconnected porous system, pore size distribution is not a well-defined parameter(Lin and Miller, 2000).

The voxel size for the previous pore geometry study of a packed bed is 17 μm. To evaluate the effectiveness of the newly installed high-resolution 3-D x-ray microtomography measurement of complex filter cake pore structure, a packed bed of iron ore particles (180x106 μm) was prepared for preliminary CT analysis. The sample was scanned using the Konoscope microtomography system. Figure 7a shows one slice from the volume data set for the packed bed of iron ore particles. A volume rendering image from a subset of this sample (256x256x128) is shown in Figure 7b. The voxel size for this sample is 10 μm. From the images in Figure 7, it evident that the resolution of the newly installed x-ray microtomography system is better than the system used in the previous study.

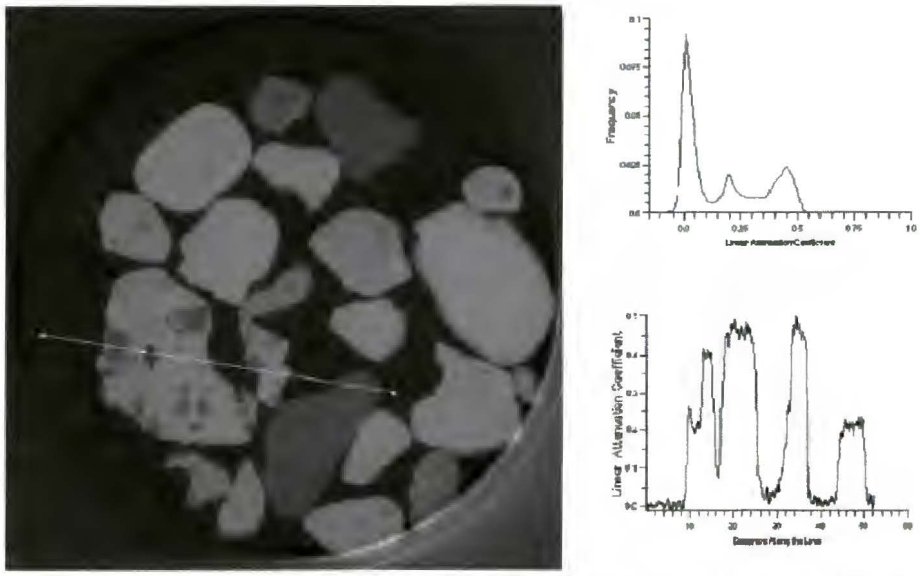

Figure 6: Based on x-ray attenuation coefficient histogram, differentiation of mineral phases within the sample is possible as shown in the upper right-hand side. Lower right-hand side shows the individual voxels along the line from the reconstructed image using x-ray microtomography

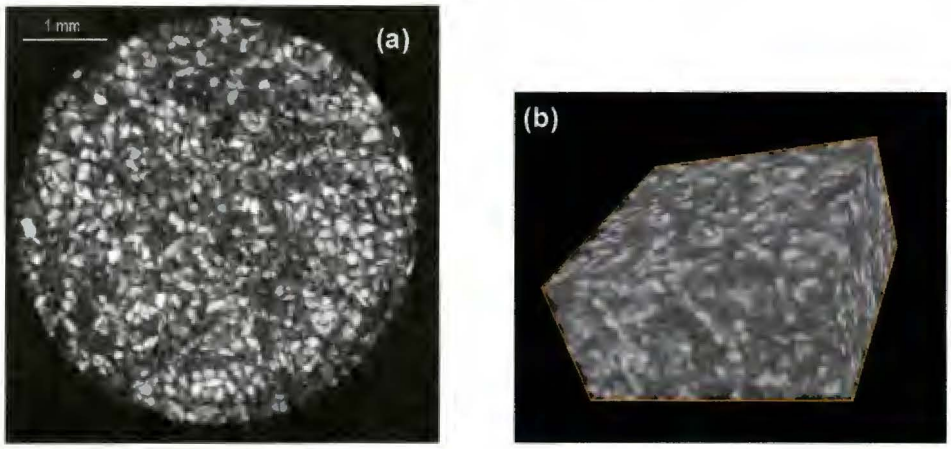

Figure 7: (a) Selected cross sectional image from a packed bed of iron ore particles (180x106 μm). (b) Volume rendering image from a subset (256x256x128) of the packed bed of iron ore particles

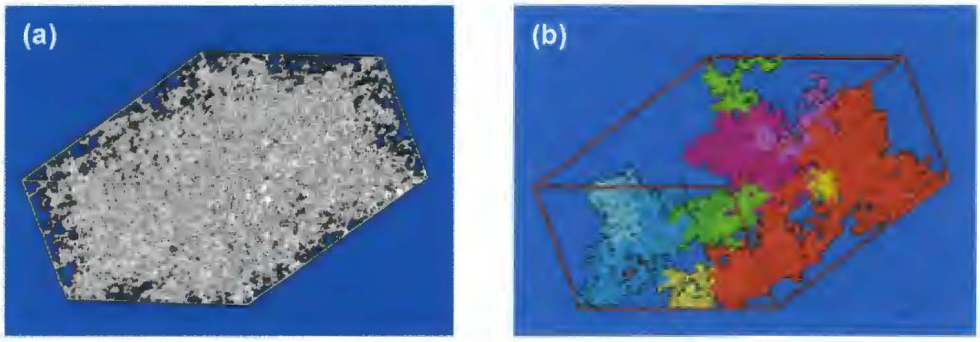

Figure 8: (a) Surface rendered image of the pore structure from a subset (256x256x128) of the 3-D MicroCT data set (Figure 7b). (b) Overall pore structure is composed with several independent major networks

Connectivity is an important concept when flow problems are considered. Fluid flow can occur between two points only when the pore space is connected. In this regard, overall pore structure is extracted from Figure 7b and the surface rendering image is shown in the Figure 8a. Results from a 3-D connection of components analysis indicates that the overall pore structure is composed with several independent major networks (Figure 8b) and some isolated pores.

3.3 Air-Void System of Concrete Structures

Entraining air in concrete imparts enhanced freeze-thaw resistance, better resistance to damage from deicers and salts, improved resistance to sulfate attack and reduced destruction due to alkali-silicate reactivity. Air entrainment is usually achieved through the use of anionic air-entraining surfactants. These air-entraining reagents adsorb at the air/water interface and act to stabilize the air bubbles and to prevent their coalescence. The air bubbles formed are dispersed in the cement during the mechanical mixing of the material. Air bubbles entrained in this way are generally between 10 and 1000 μm in diameter. Larger air bubbles (>1000 μm in diameter) are also present in all concrete due to entrapment of air during mechanical mixing. In any event, it is evident that the air-void size distribution is of particular interest. To achieve the maximum positive effect of air-entrainment, the spacing between the air bubbles is also a very important parameter and should be considered. Correct determination of the air-void system properties is of paramount importance to establish the durability of concrete particularly with respect to freeze-thaw damage.

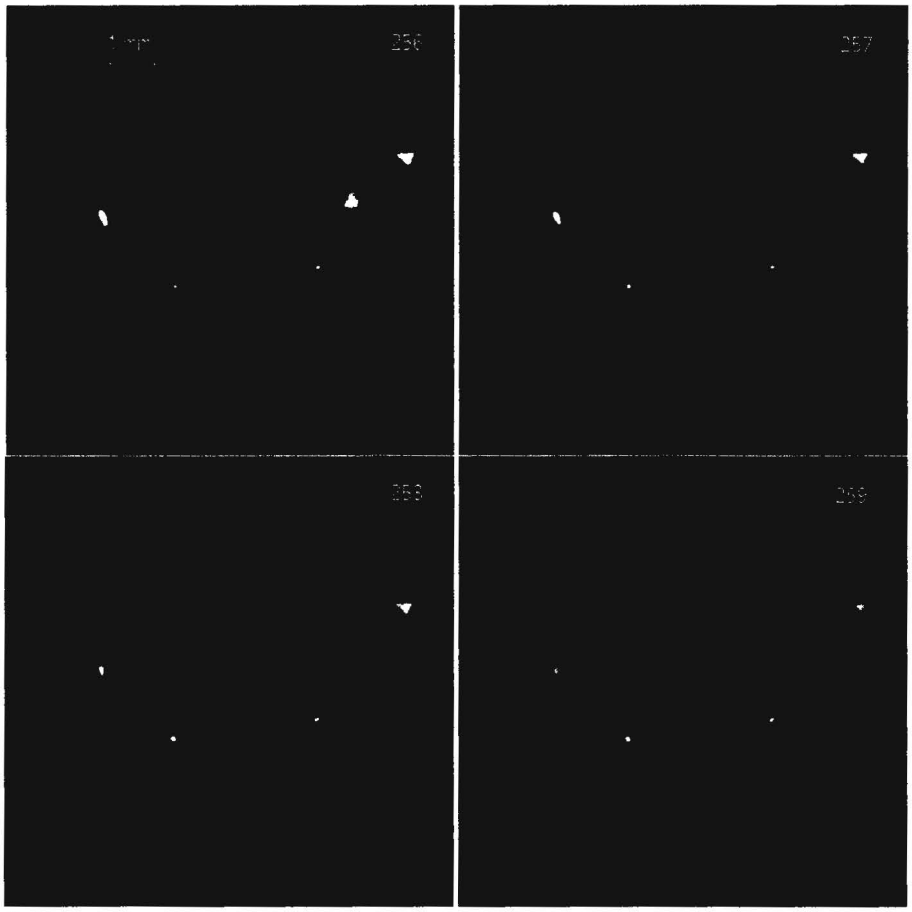

Figure 9: Cross sectional images from the three dimensional x-ray microtomography reconstruction of a concrete specimen. The dark circles reveal the air voids. The space between each of these sequential cross sectional images is 20 microns

In contrast to the traditional ASTM procedure, use of x-ray microtomography offers the opportunity for the determination of the true three-dimensional air-void size distribution. Figure 9 illustrates the ability

of the high-resolution x-ray microtomography (Konoscope) system for 3D quantitative analysis of air-voids inside the concrete structure. Four consecutive cross sections along the Z-direction are shown in Figure 9 as established from the three dimensional reconstruction of the concrete specimen.

4 CONCLUSIONS

Recently, a state-of-the-art cone beam x-ray microtomography system (Konoscope) has been installed at the University of Utah for the quantitative analysis of multiphase materials in three dimensions. This facility has been designed to obtain 2048 x 2048 pixel reconstruction over a 10-mm diameter, while allowing for the imaging of somewhat larger (40-mm) objects. The system is capable of handling high-density materials, even materials having a density as high as 8.0 g/cm^3. Details of the cone-beam x-ray microtomography system were presented. This unique, one-of-a-kind, instrument is used to obtain three-dimensional spatial reconstruction multiphase materials of irregular shape. The utilization of x-ray microtomography not only will allow for quantitative analysis of multiphase systems but also allow for textural characterization and the determination of phase continuity. Potential applications for the advanced analytical system were reviewed and include particle composition distribution (liberation analysis), pore structure analysis of packed beds, and the air-void system of concrete. Many other applications of x-ray microtomography analysis are expected including examination of microelectromechanical system (MEMS), fault mechanics and fluid transport studies, bone architecture, and multilayered ceramic composites for structural and electronic applications.

5 ACKNOWLEDGEMENTS

The authors would like to recognize NSF Grant No. CTS-9724315 which provides a major portion of the funds necessary for the design and assembly of the microCT facility.

6 REFERENCES

DUNSMUIR, J.H., FERGUSON, S.R., D;AMICO, K.L., FLANNERY, B.P. and DECKMAN, H.W., (1991), X-ray Microtomography: Quantitative Three-dimensional X-ray Microscopy, *Review of Progress in Quantitative Nondestructive Evaluation*, ed. by D.O. Thompson and D.E. Chimenti, Plenum Press, New York, Vol. 10A, pp. 443-449.

FELDKAMP, L.A. and JESION, G., (1986), Three-dimensional X-ray Computed Tomography, *Review of Progress in Quantitative Nondestructive Evaluation*, ed. by D.O. Thompson and D.E. Chimenti, Plenum Press, New York, Vol. 8A, pp. 555-566.

FLANNERY, B.P., DECKMAN, H.W., ROBERG, W.G., and D'AMICO, K.L., (1987), Three-dimensional X-ray Microtomography, *Science*, Vol. 237, pp.1439-1444.

GRODZINS, L., (1983), Optimun Energies for X-ray Transmission Tomography of Small Samples – Applications of Schnchrotron Radiation to Computerized Tomography I, *Nucl. Instrum. Meth.,* Vol. 206, pp.541-545.

KAK, A.C. and SLANEY, M., (1987), *Principles of Computerized Tomographic Imaging*, IEEE Press, New York.

KINNEY, J.H., JOHNSON, Q.C. and SAROYAN, R.A., (1988), Energy-Modulated X-ray Microtomography, *Rev. Sci. Instrum.,* 59 (1), pp. 196-197.

KINNEY, J.H., SAROYAN, R.A., and MASSEY, W.N., (1991), X-ray Tomography Microscopy for Nondestructive Characterization of Composite, *Review of Progress in Quantitative Nondestructive Evaluation,* ed. by D.O. Thompson and D.E. Chimenti, Plenum Press, New York, Vol. 10A, pp. 427-433.

LIN, C.L., MILLER, J.D. and CORTES, A.B., (1992), Applications of X-ray Computed Tomography in Particulate Systems, *KONA*, Vol. 10, pp. 88-95.

LIN. C.L. AND MILLER, J.D., (1996), Cone Beam X-ray Microtomography for three-dimensional Liberation Analysis in the 21st Century, *International Journal Of Mineral Processing*, Vol. 47, pp. 61-73.

LIN, C. L., MILLER, J. D., LUTTRELL, G. H. and ADEL, G. T., (2000), Development of an On-Line Coal Washability Analysis System Using X-ray Computed Tomography, Presented at 2000 SME Annual Meeting, Feb, Salt Lake City, Utah, Pre-print no. 00-104, 2000 and accepted to be published in *Coal Preparation*, 2001.

LIN, C.L. and MILLER, J. D., (2000), Network Analysis of Filter Cake Pore Structure by High Resolution X-ray Microtomography, *Chemical Engineering Journal*, Vol. 77, pp. 79-86.

MCCULLOUGH, E. C., (1975), Photon Attenuation in Computed Tomography, *Medical Physics*, Vol. 2, pp. 307-320.

MILLER, J.D., LIN, C.L. and CORTES, A.B., (1990), A Review of X-ray Computed Tomography and Its Applications in Mineral Processing, *Miner. Process. Extract. Metall. Rev.*, Vol. 7, pp.1-18.

WELLINGTON, S. L. and VINEGAR, H. J., (1987), X-ray Cmputerized Tomography, *J. of Petroleum Technology*, Vol. 8, pp. 885-898.